S-Band Zero-Delay Device Multipath Tests on the 64-Meter Antenna at DSS 43, DSS 63, and DSS 14

T. Y. Otoshi
Communications Elements Research Section

This article presents the results of a study to correlate the results of zero-delay subreflector tests with the multipath theory. Good agreement between theory and experiment was obtained on both S-band range and signal level data at DSS 43, DSS 63, and DSS 14. It is shown that a movable subreflector technique can be used to isolate the principal multipath errors and enable a more accurate determination of the actual ground station delay.

I. Introduction

With the exception of DSS 14, at Goldstone, California, all stations of the Deep Space Network use the conventional zero-delay ranging configuration, in which the zero-delay device (ZDD) is mounted on the paraboloidal reflector (dish) surface. A zenith range measurement via the airpath to a dish-mounted ZDD and a Z-correction (Ref. 1) provide needed ground station bias corrections for determining the true range to the spacecraft.

Results of airpath tests at DSS 14 showed that large changes in range occurred as a function of antenna elevation angle when a ZDD was mounted on the 64-m antenna dish surface (Ref. 2). Other airpath tests made on the 64-m antenna S/X system at DSS 14 showed that large range changes also occurred when small changes were made in axial focusing of the hyperboloidal subreflector. Similar type phenomena were also observed on the 64-m antenna systems at DSS 43, Canberra, Australia, and DSS 63, Madrid, Spain (Ref. 3). Since the range dependence on elevation angle could be due to a multipath phenomenon, one cannot assume that a zenith measured value is the correct value. Because of the described airpath problems, the ZDD configuration at DSS 14 has been operated in a cable configuration (Ref. 4) since January 12, 1974. However, DSS 43 and DSS 63 have continued to operate in the airpath configuration.

Because of the current range residuals of 10 to 15 meters between DSS 63 and DSS 43 for Mariner 10 results (Ref. 5), some attention has been devoted to the study of multipath as a possible cause of this discrepancy. A theory has recently been derived which results in good agreement between the multipath theory and experimental data. The purpose of this article is to present the results of some of this recent work. It will be shown that the multipath theory (with the aid of a com-

puter program) can be used to determine the true range delay of the station in the absence of multipath and thereby determine a correction to the observed station delay in the presence of multipath. Furthermore, the theory can be used to determine the physical location of the multipath source and its magnitude.

II. Theoretical Equations for Subreflector Tests

In the subreflector test, ranging measurements are performed via the airpath to a ZDD mounted on the dish surface. The test configuration may be seen in Fig. 1. The range-coded uplink signal, radiated out of the radio-frequency (RF) feed horn, is reflected off the hyperboloidal subreflector toward the dish surface. The dish-mounted ZDD horn receives a portion of this energy, and after mixing with a coherent local oscillator frequency, a coherent downlink signal is radiated back toward the hyperboloidal subreflector and reflected back toward the RF feed. The range-coded downlink signal received by the RF feed travels to the receiver system and subsequently arrives at the ranging machine.

In the ranging test, the total system round trip delay time is measured as a function of subreflector position. If the major part of the multipath signal is interacting in the region between the feed horn and the feed cone or its support structure, the subreflector movement will cause the multipath signal to go in and out of phase with the primary signal. Since the only required modification to previous theoretical work published by this author (Ref. 6) is to express the differential path length in terms of indicated subreflector position, only the equations will be presented. The derivations can be found in Ref. 6.

For the configuration of Fig. 1 the equation for two-way range can be expressed as

$$(t_g)_T = K_1 + \varepsilon_{ga} + \varepsilon_{gb} \tag{1}$$

where

K_1 = total system group delay (uplink and downlink) in the absence of multipath, s

ε_{ga} = error in the uplink delay due to multipath, s

ε_{gb} = error in the downlink delay due to multipath, s

For simplicity, assume that the primary and leakage paths are the same for the uplink and downlink signals (see Fig. 1). Then from the equations derived in Ref. 6, and assuming a free space media for both leakage and primary paths,

$$\varepsilon_{ga} = \left(\frac{(\ell_2 - \ell_1)}{c}\right) A \left(\frac{A + \cos\theta_a}{1 + 2A\cos\theta_a + A^2}\right) \tag{2}$$

$$\varepsilon_{gb} = \left(\frac{(\ell_2 - \ell_1)}{c}\right) A \left(\frac{A + \cos\theta_b}{1 + 2A\cos\theta_b + A^2}\right) \tag{3}$$

where

$$\theta_a = \frac{-2\pi f_a}{c}(\ell_2 - \ell_1) + \psi_a \tag{4}$$

$$\theta_b = \frac{-2\pi f_b}{c}(\ell_2 - \ell_1) + \psi_b \tag{5}$$

and

A = ratio of the magnitudes of the leakage and primary signals as measured at the output port of the ZDD horn (see Fig. 1)

ℓ_1, ℓ_2 = physical path lengths, respectively, of the primary and leakage paths going one-way, cm

c = speed of light ($\approx 3 \times 10^{10}$ cm/s)

f_a, f_b = uplink and downlink frequencies, respectively, Hz

ψ_a, ψ_b = phase angles of reflection coefficients (if any) in the leakage path for uplink and downlink signals, respectively, rad

The exact relationship of $(\ell_2 - \ell_1)$ to subreflector movement is difficult to derive due to defocusing effects and the changes in incidence angles that differ for the primary wave and the multipath wave. As a first-order approximation,

$$\ell_2 - \ell_1 \approx (\Delta\ell_0 + 2S_i)\,2.54 \tag{6}$$

where

$\Delta\ell_0$ = differential path length when the indicated subreflector position is zero, in.

S_i = indicated subreflector position, in.[1]

[1]The subreflector position on the equipment is indicated in inches rather than in centimeters. To be meaningful this indicated position should not be converted to the metric system.

The automatic gain control (AGC) downlink signal level change observed by the ground receiver will vary according to the relationship

$$|F_T|_{dB} = 10 \log_{10} [(1 + 2A \cos \theta_a + A^2)(1 + 2A \cos \theta_b + A^2)] \quad (7)$$

and the AGC signal level (in dBm) observed at the ground receiver is

$$AGC = K_2 + |F_T|_{dB} \quad (8)$$

where K_2 = the AGC signal level which would be observed in the absence of multipath (in dBm).

III. Theoretical and Experimental Data

A. Subreflector Tests

Figures 2 through 7 are computer printouts and plots showing a comparison of theoretical and experimental data obtained from subreflector tests at DSS 43, 63, and 14. The uplink and downlink test frequencies were approximately the Helios spacecraft frequencies of 2115 and 2297 MHz, respectively.

The printouts and plots were generated by a computer program to perform a least squares fit of theoretical values to experimental data. The theoretical data are based upon Eqs. (1) through (8), and a best fit is made first to the experimental ranging data to determine the best fit value of (1) true station delay K_1 in the absence of multipath, (2) the differential length $\Delta\ell_0$ as defined by Eq. (6), and (3) the relative strength of the leakage signal A expressed in decibels. The program then uses these best fit values of $\Delta\ell_0$ and A to calculate the theoretical AGC signal levels as a function of subreflector settings.

This sequence for best fit was chosen because the range data are a result of long term averaging, while the AGC data are either typically noisier or generally lag behind real-time changes. The AGC data are also dependent upon the accuracy of the calibration curves and operation only at the signal levels where the calibration curves apply.

Note from the computer printouts on Figs. 2, 4, and 6 that the best fit values of $\Delta\ell_0$ are typically about 3327.4 cm (1310 in.). This value compares favorably with values of approximately 3332.5 cm (1312 in.) obtained from measuring physical path lengths on scaled drawings (see table in Fig. 1). From Fig. 1, it can be seen that this value is associated with a multipath wave reflected off the cone platform. The values of approximately -15 to -20 dB for A_{dB} agree with those calculated independently by Ludwig (Ref. 7). These values are also consistent with beam efficiency values published in Ref. 8 for the portion of the beam illuminating the cone platform. An attempt to explain the higher value of about -10 dB for A_{dB} at DSS 63 will be made later after discussion of the plotted curves.

Examination of the plotted curves shows that reasonably good agreement was obtained between theory and experiment for DSS 43 and DSS 14. The typical deviations in range are about 3 ns, and typical deviations in AGC are about 0.3 dB. These deviations might be due to another smaller multipath effect caused by a wave bouncing off the cone roof and not accounted for by the theory.

The larger discrepancy for DSS 63 was previously attributed to a cone missing from the cone platform. However, it was recently learned that a cone was also missing from the cone platform on the DSS 43 antenna during 1974 and during the subreflector test. Therefore, the stronger multipath effect and larger discrepancy at DSS 63 might be due to the location of the missing cone with respect to the location of the ZDD. The ZDD locations and tricone configurations at DSS 43, DSS 63, and DSS 14 for the subreflector tests are shown in Fig. 8. Note that at DSS 63 the missing cone is at Bay 1, while at DSS 43, the missing cone is at Bay 3. Because of the different locations of the missing cone with respect to the ZDD, a stronger multipath signal could exist at DSS 63 than at DSS 43.

The large disagreement of calculated and experimental AGC values at DSS 63 can be explained as follows. The AGC calibrations at DSS 63 were performed in the region of -140 to -170 dBm while actual multipath tests were performed at -120 dBm. The measured signal levels for the tests were outside the calibrated region, and therefore the measured AGC variations were much smaller than the actual variations. G. Pasero at DSS 63 stated that when the test was repeated for AGC data only at a later date in the calibrated range of the receiver, the peak-to-peak AGC variation observed was about 10 dB. This peak-to-peak variation agrees favorably with the calculated values shown on the plots.

All of the subreflector test results presented apply only to the antenna pointed at zenith and at the S-band test frequencies involved. Results of subreflector tests at 45 and 20 deg elevation angles have been reported in Ref. 3, but as yet no curve fit has been made to these data.

B. Antenna Tipping Test

Another airpath test that is often performed is the antenna tipping test. In this test the total system range delay is continuously measured while the antenna is slowly tipped from the zenith position to the horizon. Figures 9 and 10 show the results of the tipping test for DSS 43 and DSS 63, respectively. No current tipping test data were obtained at DSS 14. The tipping tests were performed on a different day from the subreflector tests, and the measured zenith range delays differed by about 10 to 20 ns. To avoid confusion, the tipping test data were converted to show changes relative to the zenith position. A polynomial curve fit was made to the data to show trends only. The polynomial curve fit is not based on the multipath equations. However, it is interesting to note that when the antenna is tipped from the zenith position to the horizon, the subreflector moves from the normal operating point outward about 0.5 to 0.7 in. (Ref. 9). If one examines the subreflector data for DSS 43 and DSS 63, (see Figs. 3a and 5a) and moves from the operating point to a point about 0.5 in. in the positive direction, the magnitude and phase (sign) of the range change generally agree with the antenna tipping data. Therefore one can assume that the phenomena associated with the antenna tipping tests are correlated to the same multipath phenomenon observed on the subreflector test.

IV. Corrections to Measured Station Range Delay

In the preceding section it was shown that the true station delay could be determined with the aid of a computer program. The definition of true range is that which would have been measured in the absence of multipath. Since the subreflector position during pre- and post-track zero-delay calibration is known and since the true range is given by the computer program, one can calculate a correction for the measured station delay. In addition, one can predict what the observed range residuals would be between stations. For example, let

$BIAS'_{DSN}$ = measured DSS round trip delay in the *presence* of multipath

$BIAS_{DSN}$ = true DSS round trip delay in the *absence* of multipath

Using the equation in Ref. 1 the measured round-trip light time (RTLT) will be

$$RTLT' = R_{total} - BIAS_{S/C} - BIAS'_{DSN} + Z \qquad (9)$$

but the true RTLT is

$$RTLT = R_{total} - BIAS_{S/C} - BIAS_{DSN} + Z \qquad (10)$$

where R_{total} is the total measured range and Z is the Z-correction.

If $BIAS'_{DSN}$, $BIAS_{DSN}$ are given in nanoseconds the range residual in meters is computed from

$$\underset{\text{(meter)}}{\textit{Range Residual}} = [\underset{\text{(ns)}}{RTLT'} - \underset{\text{(ns)}}{RTLT}]\,[0.15] \qquad (11)$$

Substitutions of Eqs. (9) and (10) into Eq. (11) gives

$$\underset{\text{(meter)}}{\textit{Range Residual}} = [\underset{\text{(ns)}}{BIAS_{DSN}} - \underset{\text{(ns)}}{BIAS'_{DSN}}]\,[0.15] \qquad (12)$$

For DSS 43, the 1974 pre- and post-track ZDD calibrations were done with the subreflector at 0 in. Then from the data on Fig. 2

$$BIAS_{DSN} - BIAS'_{DSN} = 3198.4 - 3227.2$$
$$= -28.8\,\text{ns}$$
$$\textit{Range Residual} = -4.3\,\text{meters}$$

For DSS 63, the 1974 pre- and post-track ZDD calibrations were done with the subreflector at −0.5 in. From the data on Fig. 4,

$$BIAS_{DSN} - BIAS'_{DSN} = 4210.8 - 4155.9$$
$$= 54.9\,\text{ns}$$

and

$$\textit{Range Residual} = 8.2\,\text{meters}$$

Since DSS 14 does not operate in the airpath configuration, there is no need to compute residuals for DSS 14.

It is interesting to note that the above residuals are in excellent agreement with the residuals published by Christensen for Mariner 10 at Mercury Encounter I on March 29, 1974 (Ref. 5). Unfortunately, the results presented here cannot be used conclusively to explain the residuals. The main reason is that during Mariner 10 Mercury Encounter I on March 29, 1974, the ZDD horn at DSS 43 was located at the outer edge of the 64-m dish surface. The ZDD horn was moved to a new location closer to the center of the antenna on August 1, 1974 (see Fig. 8). The DSS 43 test results reported in this article were obtained at the new location.

Another reason why the results may not apply to the Mariner 10 residuals is the slight differences in test frequencies. If one were to assume that the same multipath conditions existed at DSS 63 as during the Mariner 10 Mercury Encounter I period, calculations show that for the Mariner 10 uplink/downlink frequencies of 2.11352 GHz/2.29523 GHz, the range residual would have been +5.0 meters. It can generally be expected that the multipath-caused residuals will change significantly with uplink/downlink frequency changes as small as 1 or 2 MHz.

Since the multipath error can change in magnitude and phase with (1) frequency, (2) ZDD horn location, or (3) the RF feed configuration, it is important to document these parameters for future reference. The test configurations for the tests done at DSS 43, DSS 63, and DSS 14 are shown in Fig. 8. Table 1 shows the critical parameters of interest which if altered would invalidate the range correction data obtained.

V. Summary and Recommendations for Future Work

It has been shown that even though multipath effects are present on the antenna, the effect can be separated out by the movable subreflector technique. This method assumes that the dominant interaction is occurring between the subreflector and the cone or its support structure. If there are multipath effects outside this region, one must use a movable ZDD horn on the dish surface such as that described in Ref. 6. Range measurements made over a band of frequencies might also reveal multipath effects and enable identification of multipath sources.

If the station periodically (every 3 months) obtains data from the subreflector test, then through the use of the computer program, one could determine the station delay more accurately. Since the computer program also assists in locating the multipath source, a simple antenna redesign might be done to eliminate the problem entirely. One solution may be to restore the hyperboloid vertex plate which is not present on 64-m antennas.

Although good agreement was obtained between theory and experiment for the tests described in this article, it is still desirable to confirm the location of multipath source. Plans are being made to perform an experiment placing absorbers on the cone platform of the DSS 14 64-m antenna and seeing if the dominant multipath effect disappears for both S- and X-band. The results of this test will be reported in a future issue of this publication.

References

1. *TRK-2-8 Module of DSN System Requirements Detailed Interface Design Document 820-13, Rev. A,* Jet Propulsion Laboratory, Pasadena, Calif., July 1, 1973 (an internal document).
2. Stelzried, C. T., Otoshi, T. Y., and Batelaan, P. D., "S/X Band Experiment: Zero Delay Device Antenna Location," in *The Deep Space Network Progress Report 42-20,* pp. 64–68, Jet Propulsion Laboratory, Pasadena, Calif., Apr. 15, 1974.
3. Otoshi, T. Y., and LuValle, J., "Zero Delay Device Airpath Tests at DSS 43 and 63," IOM 3333-75-048, Jet Propulsion Laboratory, Pasadena, Calif., Apr. 1, 1975 (an internal document).
4. Otoshi, T. Y., and Stelzried, C. T., "S/X Experiment: A New Configuration for Ground System Range Calibrations With the Zero Delay Device," in *The Deep Space Network Progress Report 42-20,* pp. 57–63, Jet Propulsion Laboratory, Pasadena, Calif., Apr. 15, 1974.

References (contd)

5. Christensen, C., "Corrected Mariner 10 Range Residuals," IOM 391.8-268, Jet Propulsion Laboratory, Pasadena, Calif., Apr. 24, 1975 (an internal document).

6. Otoshi, T. Y., "S/X Band Experiment: A Study of the Effects of Multipath on Two-Way Range," in *The Deep Space Network Progress Report 42-25*, pp. 69–83, Jet Propulsion Laboratory, Pasadena, Calif., Feb. 15, 1975.

7. Ludwig, A. C., "Multipath Calculations for Range Error Calibration Probe," IOM 3333-75-161, Jet Propulsion Laboratory, Pasadena, Calif., Aug. 22, 1975 (an internal document).

8. Bathker, D. B., *Predicted and Measured Power Density Description of a Large Ground Microwave System*, Technical Memorandum 33-433, Jet Propulsion Laboratory, Pasadena, Calif., Apr. 15, 1971. See Eta S Column in Table II, p. 31.

9. Katow, M. S., "64-m Subreflector–Gravity Deflections," IOM 3324-75-136, Jet Propulsion Laboratory, Pasadena, Calif., Sept. 2, 1975 (an internal document).

Acknowledgments

The author would like to acknowledge the assistance of J. LuValle of Network Operations in writing the test procedure for overseas station tests. Splendid cooperation was obtained from G. Pasero of DSS 63 and R. Denize of DSS 43, who took the data and furnished additional details about the test configurations. H. Marks of Informatics wrote the Engineering Calibration Program used in the tests and has made the program tapes and documentation available to all stations in the Network. T. Cullen of the Communications Elements Research Section wrote the sophisticated computer program that enabled the theoretical portion of this work to be successful. The subreflector technique was originally suggested by Dr. R. W. Beatty, Consulting Electronics Engineer, for purposes of checking ranging system measurement accuracy. His suggested subreflector tests subsequently led to the discovery of the multipath phenomenon.

Table 1. Multipath test configuration and tabulation of critical multipath-dependent parameters

DSS	Test frequencies, GHz		Normal subreflector operating position, in.	ZDD horn location	S-band cone	S/X dichroic plate installed	Approximate period for which test results are valid
	Uplink	Downlink					
43	2.115770	2.297670	0	Dish surface as indicated on Fig. 8	SPD	No	August 1, 1974 (new horn location) to February 13, 1975 (when XRO[a] cone and S/X feed installed)
63	2.115700	2.297593	−0.5 (0.5 in. IN)	Dish surface as indicated on Fig. 8	SPD	No	Throughout 1974 to February 1975 (when S/X feed installed)
14	2.115650	2.297540	−0.5 (0.5 in. IN)	Box on side of Mod III section on same level as cone platform (Fig. 8)	SPD	Yes	March 19, 1975 when SPD[b] cone/ XRO cone installed) to present

[a]X-band receive only.

[b]S-band polarization diversity.

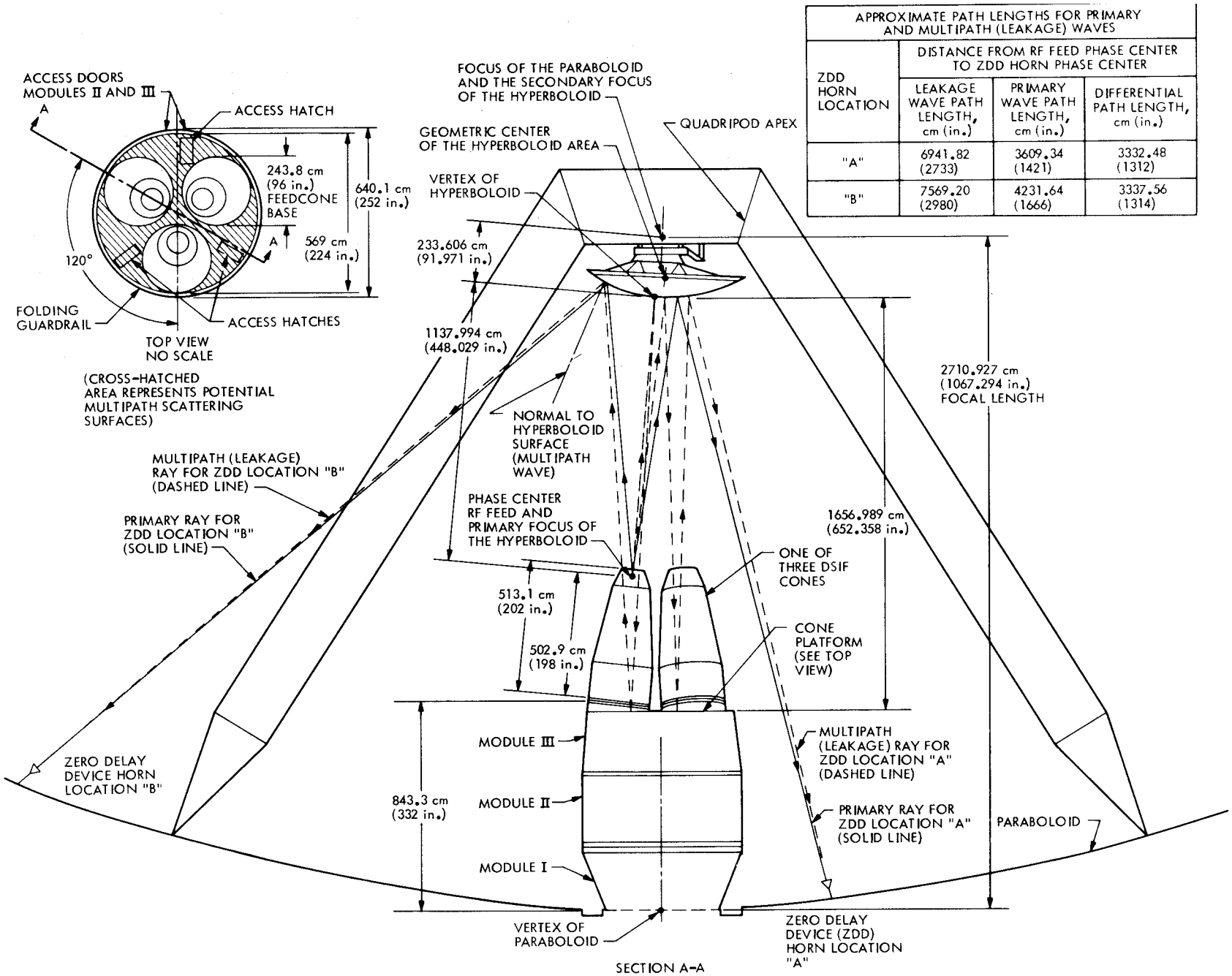

APPROXIMATE PATH LENGTHS FOR PRIMARY AND MULTIPATH (LEAKAGE) WAVES			
ZDD HORN LOCATION	DISTANCE FROM RF FEED PHASE CENTER TO ZDD HORN PHASE CENTER		
	LEAKAGE WAVE PATH LENGTH, cm (in.)	PRIMARY WAVE PATH LENGTH, cm (in.)	DIFFERENTIAL PATH LENGTH, cm (in.)
"A"	6941.82 (2733)	3609.34 (1421)	3332.48 (1312)
"B"	7569.20 (2980)	4231.64 (1666)	3337.56 (1314)

Fig. 1. 64-m antenna geometry for multipath tests

DSS 43 SUBREFL TESTS AT ZENITH, 1974 GMT DAY 362

FA= 2.115770 GHZ FB= 2.297670 GHZ

ADBL=-24.0000 DB ADBU=-15.0000 DB

DLZL= 1295.000 INCH DLZU= 1325.000 INCH

SUBREF POSITION (INCH)	EXPER. RANGE DELAY (NS)	CALC. RANGE DELAY (NS)	RANGE DIFF. (NS)	EXP AGC (DBM)	CALC AGC (DBM)	AGC DIFF. (DB)
-3.000	3226.80	3223.15	3.646	-121.14	-120.72	-.421
-2.500	3227.90	3227.77	.126	-120.00	-120.25	.252
-2.000	3202.20	3203.23	-1.028	-122.34	-122.47	.135
-1.500	3162.60	3164.89	-2.286	-125.59	-125.20	-.385
-1.000	3171.20	3174.40	-3.203	-125.22	-124.55	-.668
-.500	3210.80	3211.96	-1.164	-121.98	-121.70	-.272
.000	3227.20	3226.98	.220	-119.87	-120.35	.481
.500	3210.40	3212.25	-1.845	-121.07	-121.66	.586
1.000	3181.40	3178.36	3.040	-124.05	-124.21	.165
1.500	3178.60	3172.65	5.954	-124.55	-124.70	.155
2.000	3195.50	3196.94	-1.440	-122.81	-122.79	-.026

BEST FIT VALUES FOR OPTION 1

	K1 (NS)	ADB (DB)	DLZ (INCH)	K2 (DBM)
FIRST ESTIMATE	3198.51	-15.45	1311.500	
FINAL ESTIMATE	3198.41	-15.38	1311.286	-122.6793

Fig. 2. Sample printout of computer program for DSS 43 subreflector tests

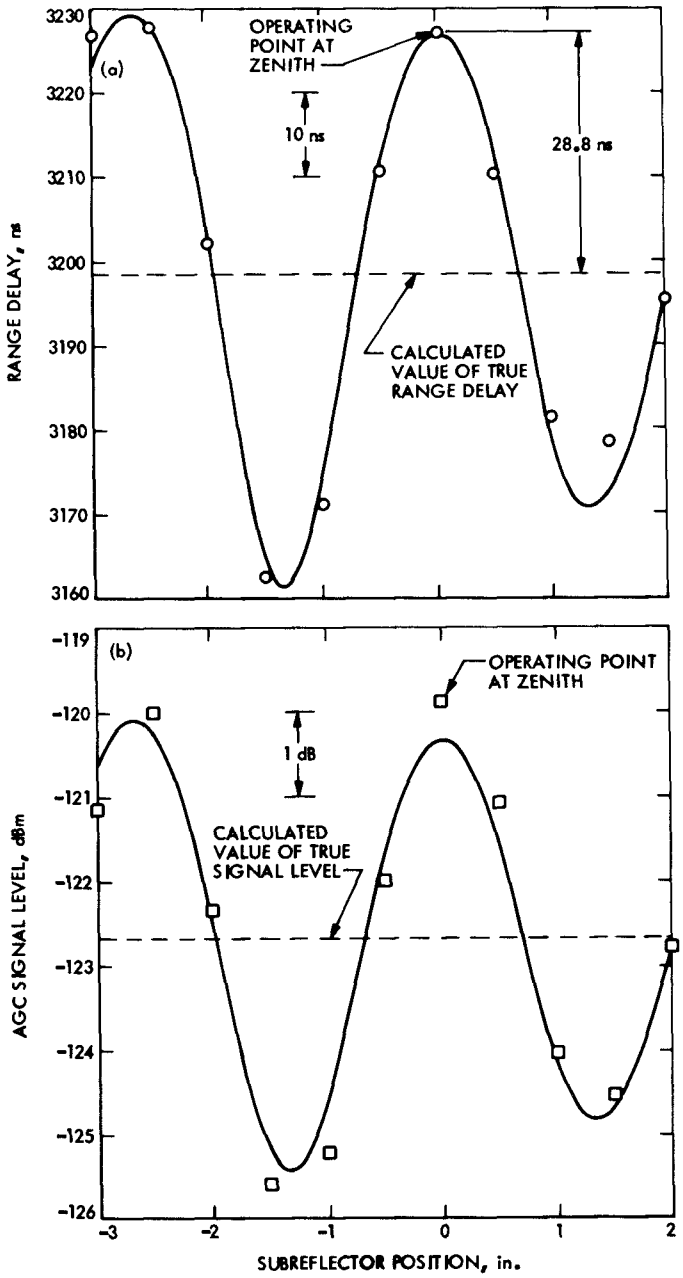

Fig. 3. Comparison of theoretical and experimental results for subreflector tests at DSS 43 on 1974 GMT Day 362 (zenith measurement): (a) Range delay, (b) Downlink received signal level

DSS 63 SUBREFL TESTS AT ZENITH, 1975 GMT DAY 29

FA= 2.115700 GHZ FB= 2.297593 GHZ

ADBL=-24.0000 DB ADBU=-12.0000 DB

DLZL= 1295.000 INCH DLZU= 1325.000 INCH

SUBREF POSITION (INCH)	EXPER. RANGE DELAY (NS)	CALC. RANGE DELAY (NS)	RANGE DIFF. (NS)	EXP AGC (DBM)	CALC AGC (DBM)	AGC DIFF. (DB)
-3.000	4217.20	4198.45	18.746	-127.47	-129.64	2.173
-2.500	4258.40	4255.99	2.415	-127.27	-124.21	-3.057
-2.000	4253.10	4263.42	-10.317	-127.27	-123.17	-4.105
-1.500	4213.30	4235.41	-22.106	-127.30	-126.62	-.677
-1.000	4122.60	4134.17	-11.572	-128.25	-133.43	5.186
-.500	4155.90	4159.18	-3.278	-128.16	-132.18	4.020
.000	4253.30	4245.23	8.070	-127.33	-125.58	-1.748
.500	4276.90	4264.77	12.128	-127.27	-122.99	-4.275
1.000	4256.10	4250.93	5.169	-127.27	-124.90	-2.373
1.500	4201.10	4178.04	23.064	-127.67	-131.02	3.352
2.000	4122.40	4121.87	.534	-128.69	-133.94	5.247
2.500	4201.70	4223.11	-21.406	-127.71	-127.68	-.026
3.000	4259.60	4261.05	-1.446	-127.28	-123.56	-3.718

BEST FIT VALUES FOR OPTION 1

	K1 (NS)	ADB (DB)	DLZ (INCH)	K2 (DBM)
FIRST ESTIMATE	4215.10	-12.00	1299.500	
FINAL ESTIMATE	4210.83	-9.74	1299.573	-127.8646

Fig. 4. Sample printout of computer program for DSS 63 subreflector tests

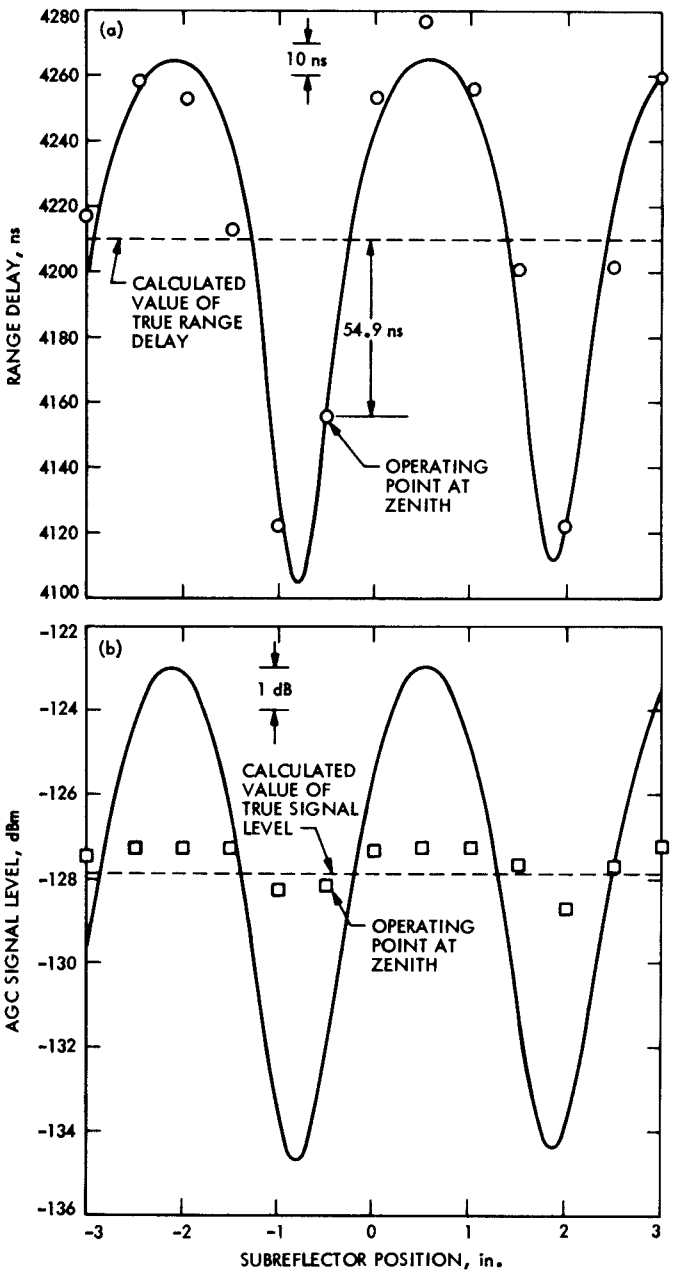

Fig. 5. Comparison of theoretical and experimental results for subreflector tests at DSS 63 on 1975 GMT Day 29 (zenith measurement): (a) Range delay, (b) Downlink received signal level

HELIOS PASS 215 POST CAL DSS 14, 1975 GMT DAY 193

FA= 2.115650 GHZ FB= 2.297540 GHZ

ADBL=-24.0000 DB ADBU=-15.0000 DB

DLZL= 1295.000 INCH DLZU= 1325.000 INCH

SUBREF POSITION (INCH)	EXPER. RANGE DELAY (NS)	CALC. RANGE DELAY (NS)	RANGE DIFF. (NS)	EXP AGC (DBM)	CALC AGC (DBM)	AGC DIFF. (DB)
-3.000	3276.20	3272.74	3.465	-135.64	-135.57	-.070
-2.500	3255.90	3261.34	-5.442	-136.50	-136.34	-.163
-2.000	3286.10	3285.53	.574	-134.68	-134.61	-.066
-1.500	3304.30	3305.28	-.983	-132.40	-132.93	.532
-1.000	3305.30	3304.02	1.275	-132.73	-133.05	.318
-.500	3279.60	3282.72	-3.118	-134.88	-134.81	-.071
.000	3266.50	3263.51	2.995	-136.14	-136.19	.051
.500	3276.60	3275.99	.605	-135.32	-135.29	-.026
1.000	3295.00	3298.83	-3.834	-133.22	-133.50	.277
1.500	3306.70	3305.02	1.685	-132.75	-132.97	.217
2.000	3289.00	3290.37	-1.370	-134.72	-134.17	-.548
2.500	3266.60	3270.71	-4.107	-136.36	-135.67	-.687
3.000	3278.70	3271.84	6.856	-135.35	-135.59	.236

BEST FIT VALUES FOR OPTION 1

	K1 (NS)	ADB (DB)	DLZ (INCH)	K2 (DBM)
FIRST ESTIMATE	3286.38	-19.05	1308.500	
FINAL ESTIMATE	3286.46	-19.15	1308.580	-134.4510

Fig. 6. Sample printout of computer program for DSS 14 subreflector tests

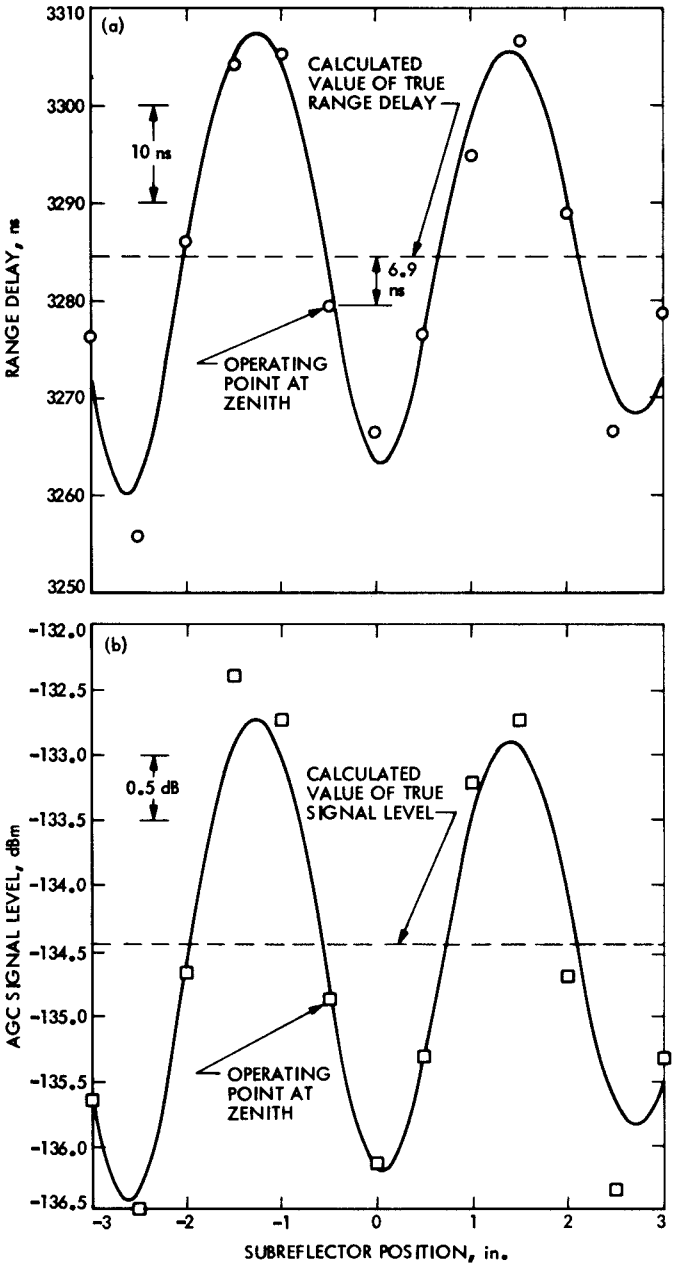

Fig. 7. Comparison of theoretical and experimental results for subreflector tests at DSS 14 on 1975 GMT Day 193 (zenith measurement): (a) Range delay, (b) Downlink received signal level

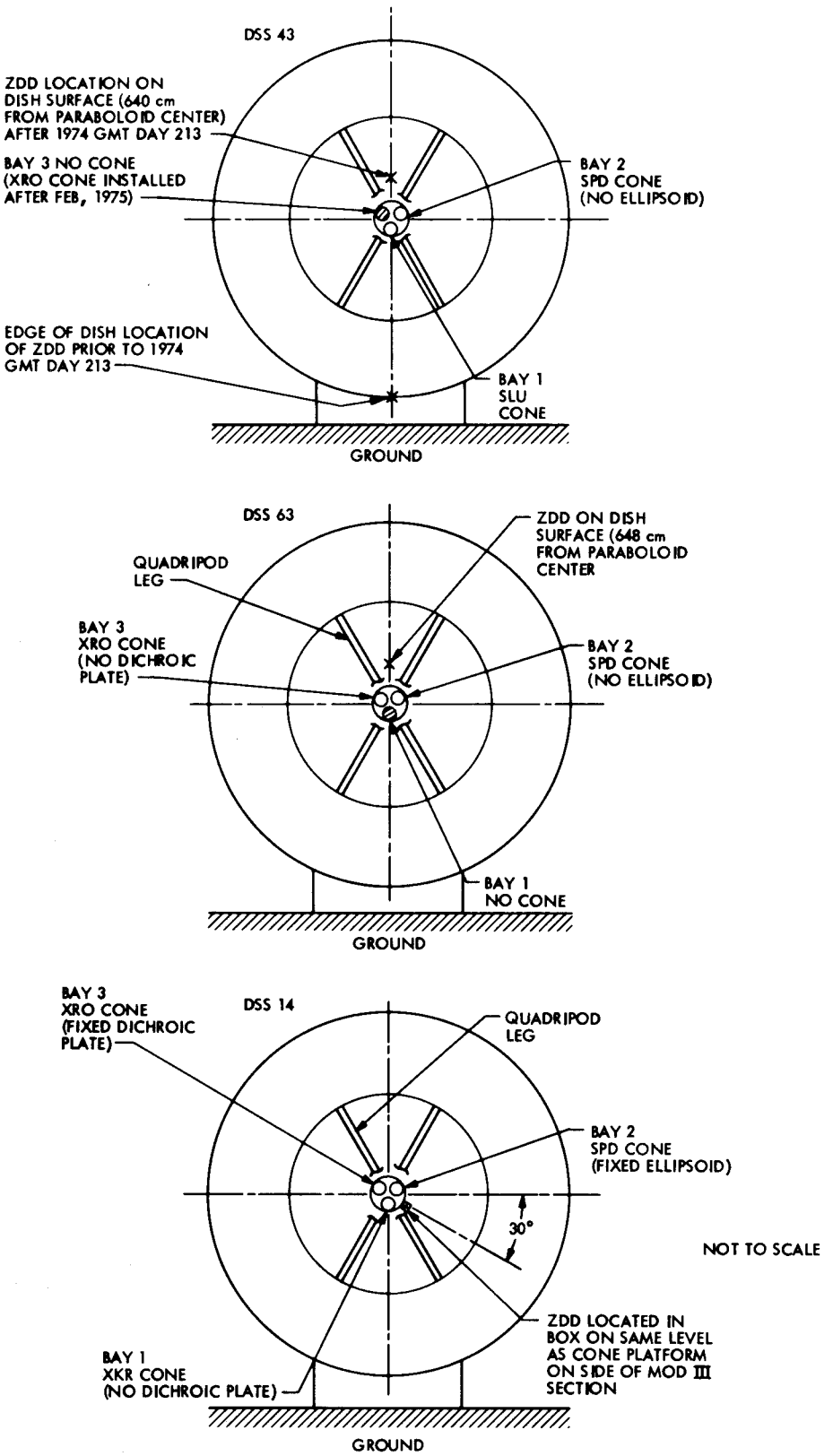

Fig. 8. DSS 43, DSS 63, and DSS 14 zero-delay device locations and tricone configuration for subreflector tests

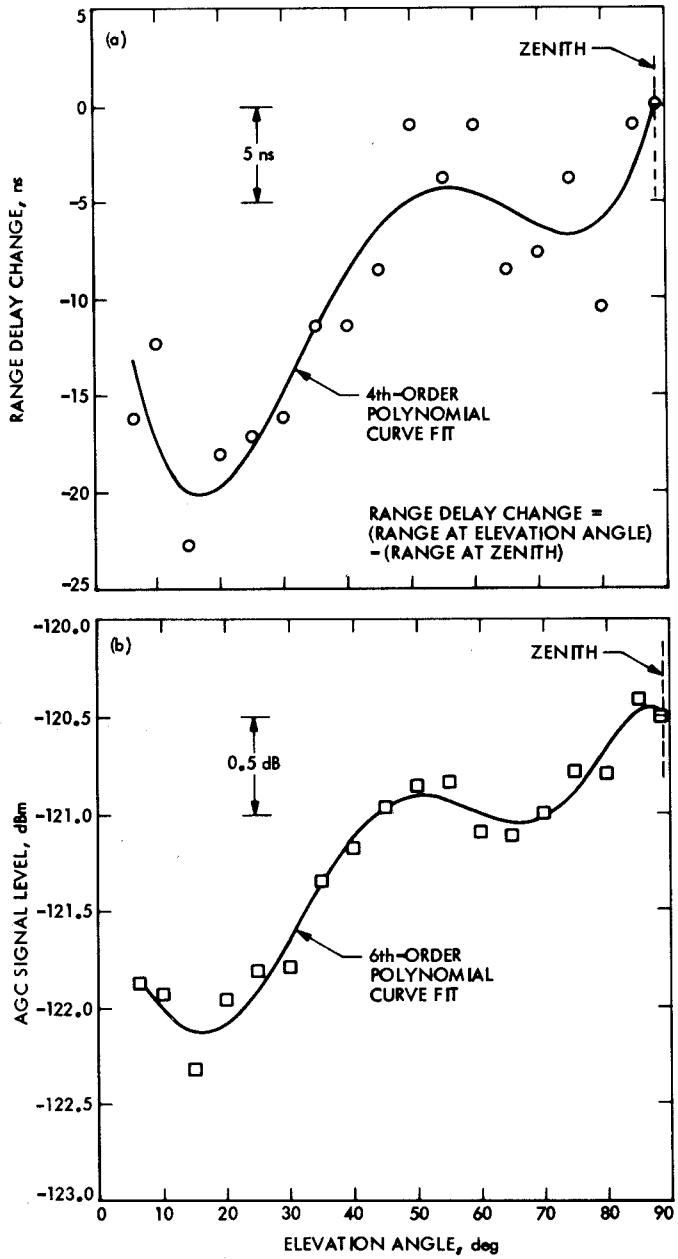

Fig. 9. DSS 43 antenna tipping tests at S-band, 1974 GMT Day 359: (a) Range delay change, (b) Downlink received signal level

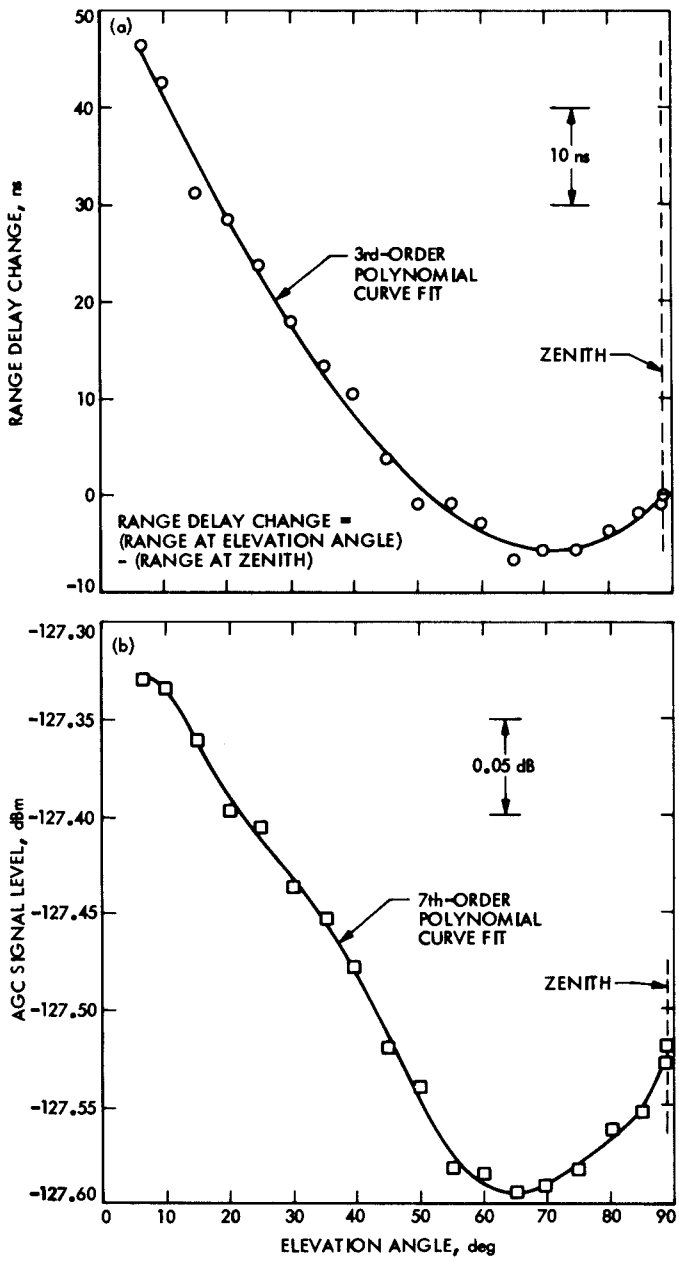

Fig. 10. DSS 63 antenna tipping tests at S-band, 1975 GMT Day 27: (a) Range delay change, (b) Downlink received signal level